Molecular Mechanism of Clinically Oriented Drug Famotidine with the Identified Potential Target of SARS-CoV-2

Parth Sarthi Sen Gupta[1], Satyaranjan Biswal[1], Dipankar Singha[1], and Malay Kumar Rana[1*]

[1]Department of Chemical Sciences, Indian Institute of Science Education and Research (IISER) Berhampur, 760010 Odisha.

[*]**Corresponding Author**

Dr. Malay Kumar Rana,

Assistant Professor,

Department of Chemical Sciences,

Indian Institute of Science Education and Research (IISER) Berhampur,

Ganjam, Odisha, 760010, India

Email: mrana@iiserbpr.ac.in

Mobile: +91-680-2227753

Abstract

Due to the current pandemic nature, severity, and rapid spread of COVID-19, there is eminent need to identify potential therapeutics to inhibit the novel coronavirus. In the quest, scientists from the USA had reported that the use of Famotidine in patients was associated with improved clinical outcomes and a reduced risk of intubation or death from COVID-19. However, the exact mode of action, the binding mechanism, and precise COVID-19 molecular target with which Famotidine interacts are yet to be ascertained. Here, 12 different COVID-19 protein targets have been screened against Famotidine employing molecular docking and molecular dynamics simulation. This reveals, among all the targets, the Papain-like protease (PLpro) as the potential target having the strongest affinity to Famotidine estimated to be of -7.9 kcal/mol with three hydrogen bonds. Tyrosine residue in the 268th position in the binding site seems to be very crucial for the stability of the PLpro-Famotidine complex, giving rise to multiple interactions such as hydrogen bonding as well as π-Sulfur. While the post-molecular dynamics (MD) analyses such as the root-mean-square deviation (RMSD) and fluctuation (RMSF), the radius of gyration (R_g), and the principal component analysis (PCA) affirm the stability of the complex providing an insight into the binding mechanism, the identification of a valid target PLpro of SARS-COV-2 for Famotidine would help understand its action, further development, and experimental exploration.

Keywords: Molecular docking, Molecular dynamics, Famotidine, COVID-19, PLpro

1. Introduction

The coronavirus SARS-CoV-2 (previously known as nCoV-19), declared pandemic by the World Health Organization (WHO) (Cucinotta *et al*., 2020), as of now has infected more than 5 million individuals and has claimed the lives of more than 328,000 people across 212 countries globally. The coronavirus pandemic (COVID-19) has been associated with acute respiratory distress syndrome resulted from an enveloped, positive-sense, single-stranded RNA beta-coronavirus that has a genome of over 29 kb in length (Prajapat et al., 2020; Sarma *et al*., 2020). Six members of the *Coronaviridae* family were previously known to infect humans,

including severe acute respiratory syndrome coronavirus (SARS-CoV) and Middle East respiratory syndrome coronavirus (MERS-CoV), in 2002 and 2012, respectively. SARS-CoV-2 is the latest addition to the family and has less severe symptoms and a lower mortality rate (6.4%), but more infectious (Zhu *et al*., 2020; Muralidharan *et al*., 2020; Gupta *et al*., 2020) than the SARS-CoV and MERS-CoV with the fatality rate of 10% and 36%, respectively (Chang *et al*., 2006). An increasing number of infections and the death toll despite concerted efforts to contain the pandemic using various strategies, ushers an adverse global impact on health and economics (Petropoulos *et al*., 2020), impelling to discover preventive therapeutics as quickly as possible. The scenario is further made worst by the fact that at present, no clinically effective drug has been approved for the treatment of this virus infection.

Target-identification and mechanism-of-action studies of effective drugs have important roles in drug discovery (Schenone *et al*., 2013). SARS-COV-2 has several non-structural and structural proteins such as matrix protein (M protein), small envelop protein (E protein), trimeric spike (S) glycoprotein, nucleocapsid protein (N protein), Main protease (Mpro), Papain-like protease (PLpro), Nonstructural protein (nsp) 13 (helicase), nsp12 (RNA-dependent RNA polymerase, RdRp), nsp14 (N-terminal exoribonuclease and C-terminal guanine-N7 methyl transferase), nsp15 (Uridylate-specific endoribonuclease), nsp16, (2'-O-methyltransferase), and nsp10 (Wu et al., 2020; Li et al., 2020; Kong et al., 2020). These proteins can be the potential targets for the novel or repurposed drug discovery.

The two proteases of SARS-CoV-2, chymotrypsin like protease (3CLPro) and Papain-like protease (PLpro), are necessary for the viral survival (Li et al., 2020). These two proteases are responsible for the cleavage of SARS-CoV-2 encoded polyprotein1a/b (PP1 a/b) resulting in multifunctional proteins involved in transcription, replication, and infection of the virion. PLpro cleaves the starting three sites at the N-terminus and 3CLpro cleaves other remaining 11 sites of PP1 a/b forming 16 non-structural proteins (Kiemer et al., 2004; Ratia et al., 2006). SARS-CoV-2 PLpro aids in replication as well as subverts cellular ubiquitination machinery to facilitate viral survival. Because of the crucial roles in the viral replication and survival, PLpro is a promising drug target for SARS-CoV-2.

Famotidine is a histamine-2 receptor antagonist that blocks the action of histamine in the parietal cells, ultimately blocking acid secretion in the stomach (Freedberg et al., 2020). It is

frequently prescribed for hospitalized patients for stress ulcer prophylaxis, gastroesophageal reflux disease, and Zollinger-Ellison syndrome (Sekiguchi et al., 1987; Freedberg et al., 2020). Recently, scientists from the USA have reported that the use of Famotidine in 1,620 hospitalized patients with COVID-19 was associated with improved clinical outcomes and a reduced risk of intubation or death (Freedberg et al., 2020). In the past, Famotidine has demonstrated its i*n vitro* antiviral properties by inhibiting the replication of HIV (Bourinbaiar et al., 1996). With a lack of further details as to how Famotidine inhibiting the virus, the exact mechanism and the target in which Famotidine interacts with SARS-CoV-2 is yet to be identified. Such information can proliferate the identification and design of more powerful drugs than Famotidine against SARS-CoV-2 in the near future.

Therefore, in the present study, we explore the interaction between all possible targets of COVID-19 with Famotidine, providing a molecular insight to identify the specific target to which this drug is most likely to bind. Molecular docking of Famotidine with twelve SARS-COV-2's targets was carried out to identify the potential target. Further, molecular dynamics (MD) simulation and post-dynamics analysis, such as RMSD, RMSF, Rg, hydrogen bond, and principal component analysis (PCA) to understand the stability and binding mechanism of the complex of Famotidine with the best targets were performed. The effectiveness of Famotidine in the clinical trial and wide availability of the drug provide hope to combat the novel coronavirus. Thus, the focus of this work on the target-identification and manifestation of the binding mechanism would provide necessary information to the researcher for further exploration in the potential therapeutic discovery against the SARS-CoV-2 pandemic.

2. Materials and Methods

2.1 Protein and ligand structure preparation

The twelve targets of SARS-COV-2 used in the study are four structural targets: matrix protein (M protein), small envelop protein (E protein), trimeric spike (S) glycoprotein, nucleocapsid protein (N protein), and eight non-structural targets: two proteases, namely Main protease (Mpro) and Papain-like protease (PLpro), nsp13 (helicase), nsp12 (RNA-dependent RNA polymerase, RdRp), nsp14 (N-terminal exoribonuclease and C-terminal guanine-N7 methyl transferase), nsp15 (Uridylate-specific endoribonuclease), nsp16 (2'-O-methyltransferase), and pnsp10, (Kong et al., 2020) (**Figure S1** in the supporting information). The 3D structures

wherever available were retrieved from the RCSB database, otherwise, the structures were modelled using Modeller (Kong et al., 2020) followed by validation and energy minimization with GROMACS. The 3D structure of PLpro with PDB ID 6W9C was used in this study. The structure of Famotidine was retrieved from Drug Bank (Wishart et al., 2018) followed by geometry optimization using Gaussian 16 at the level DFT/B3LYP/6-31+G(d, p).

2.2 Molecular docking

COVID-19 docking server (Kong et al., 2020) was utilized for the the initial docking of Famotidine with twelve targets which was later verified by manual docking using AutoDock Vina (Trott et al., 2010). For docking, after removal of water, the Kollman charges were added to the protein targets. Similarly, fixing of missing hydrogens, assignment of the Gasteiger charges and rotatable bonds were performed to Famotidine. Next, Famotidine was docked with the 12 target proteins using AutoDock Vina. For sequential docking, the autogrid size was set to specific binding regions of each target with the default grid spacing. Lamarckian Genetic Algorithm (GA 4.2) was used for the docking. Top 10 docking scores and corresponding poses were analyzed by the Discovery Studio visualizer. The best-docked complex, PLpro-Famotidine, was subjected to the molecular dynamics simulation study.

2.3 MD simulation

MD simulations were carried out for the PLpro-Famotidine complex and only PLpro (for comparison) for a period of 50 ns using GROMACS (GROningenMAchine for Chemical Simulations) v5.1 (Pronk et al., 2013). The unit cell defined as a cubical box, with a minimal distance of 10 Å from the protein surface to the edges of the box, was solvated using the Simple Point Charge (SPC) water model; the topologies of these selected targets and Famotidine were created by the GROMOS96 53a6 force field (Oostenbrink et al., 2004). Counter-ions were added to make every system electrically neutral at a salt concentration of 0.15 mol/L. Before the MD run, each system was subjected to energy minimization by employing the steepest descent integrator for 5000 steps with force convergence of <1000 kcal mol^{-1} nm^{-1}.

Thereafter, each protein-ligand complex was equilibrated for 5 ns using the canonical (NVT) and the isothermal-isobaric (NPT) ensembles. During equilibration, each system was coupled with the Berendsen temperature and the Parrinello-Rahman pressure controllers, respectively,

to maintain a temperature of 300 K and pressure 1 bar. The Particle Mesh Ewald (PME) algorithm (Essmann et al., 1995) was employed to deal with the long-range Coulomb interactions with a Fourier grid spacing of 0.12 nm. The short-range van der Waals interaction was given by the Lennard-Jones potential with a cut-off distance of 1 nm. All bond lengths were constrained by the linear constraint solver (LINCS) method (Hess et al., 1997).

Subsequently, 50 ns production run was performed under the micro-canonical ensemble by relaxing the couplings with the thermostats. In principle, the same protocol was applied to both systems. A time step of 2 fs was used and the coordinates were saved at every 10 ps during the production run. For the structural analyses of every system, the resultant MD trajectories were analyzed using the built-in modules of GROMACS and visual molecular dynamics (VMD 1.9.1). The 2D plots depicting the intrinsic dynamical stabilities captured by the root-mean-square deviation (RMSD), root-mean-square fluctuation (RMSF), radius of gyration (R_g), hydrogen bond, and principal component analysis (PCA) like our previous studies (Sen Gupta et al., 2020; Singh et al., 2020) of the complexes were generated by the Grace 5.1.23 program.

3. Results and discussion

3.1 Molecular docking and binding mode analysis

Molecular docking and dynamics are the core part of designing, screening and identification of new bioactive molecules as well as protein targets (Schenone *et al*., 2013). Molecular docking of Famotidine with the twelve targets of SARS-CoV-2 was performed and the rank (descending order) according to their binding energies with Famotidine is **Papain-like protease (**ΔG = -7.90**) >** RNA dependent RNA polymerase (RdRp) with RNA (ΔG = -7.00) = Nsp14(N7-MTase) **(**ΔG = -7.00**) >** RdRp without RNA (ΔG = -6.80) **>** Nsp16(2'-O-MTase) **(**ΔG = -6.50**) =** Nsp14(Exon) (ΔG = -6.50) > N protein NCB site **(**ΔG = -6.30**) >** Nsp15(endoribonuclease) (ΔG = -6.10) **>** Main Protease **(**ΔG = -6.00**) >** Helicase ADP site (ΔG = -5.90) **>** Helicase NCB site (ΔG = -5.60 **>** E protein (ion channel) **(**ΔG = -4.60**)**, please see **Figure 1** and **Table S1** in the supporting information), all ΔGs are in kcal/mol.

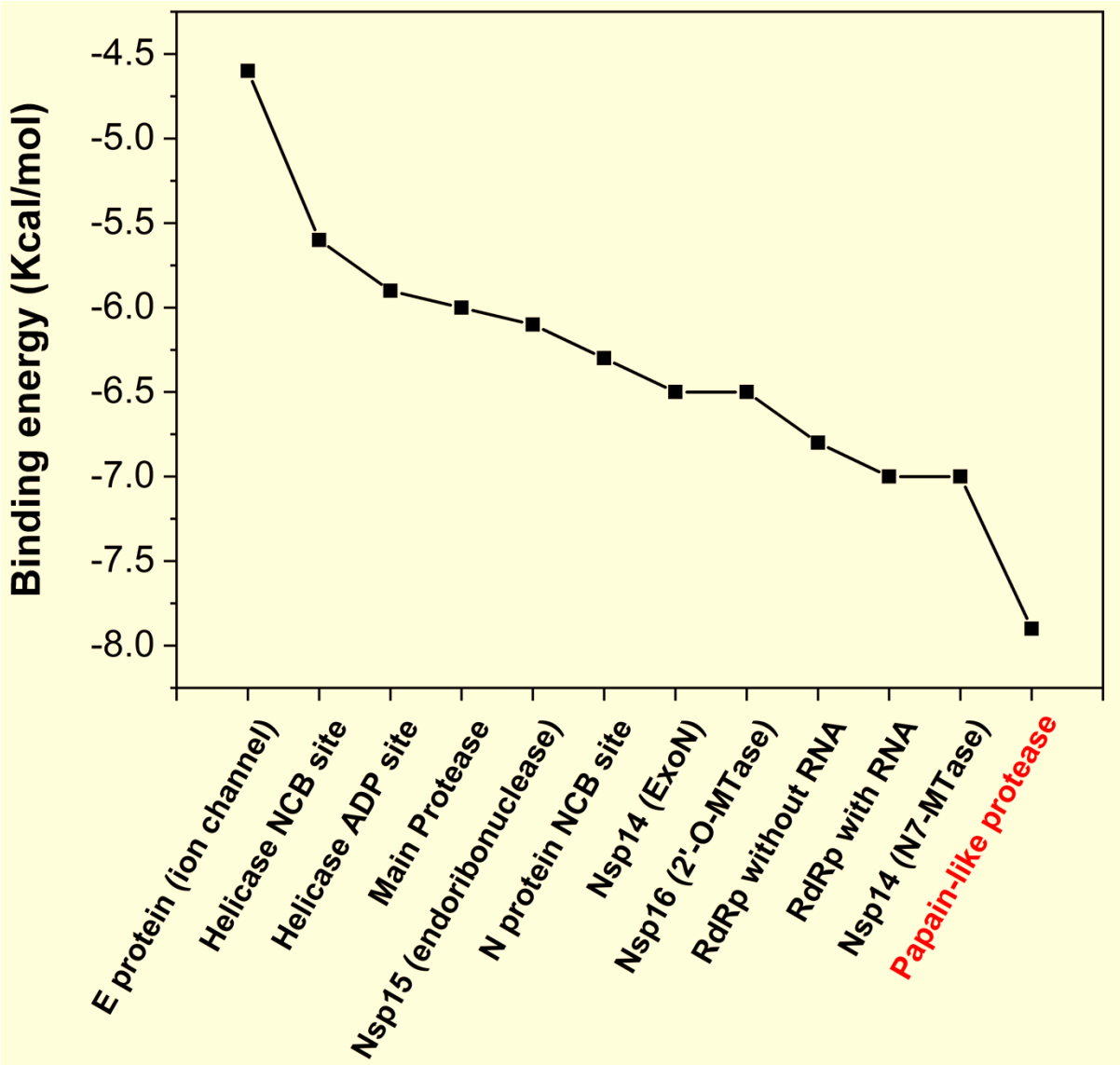

Figure 1: Binding energies (in kcal/mol) of Famotidine with twelve COVID-19 (SARS-COV2) targets selected in this study. The Papain-like protease having the lowest binding energy is shown in red color.

Among all 12 targets, the Papain-like protease (PLpro) has the best docking score with Famotidine having a binding energy of -7.90 kcal/mol, followed by Nsp14 (N7-MTase) and RdRp with RNA (both having -7.00 kcal/mol binding energy) **(Figure 1)**. PLpro having the lowest binding energy and thereby the highest docking score is considered for further study to get insights into its binding mechanism and stability with Famotidine. Recently, in an article published in Nature Medicine (Shaffer, L., 2020), the authors hypothesized that PLpro might be

the potential target for Famotidine, however, any study which could confirm the hypothesis and the mechanism of action of Famotidine did not exist until the current study is carried out.

The genome of SARS-CoV-2, structure of the PLpro-Famotidine complex, and the amino acid residues of PLpro interacting with Famotidine contributing to the aforesaid docking score are shown in **Figures 2A, 2B, and 2C**, respectively. The genome accounts for fourteen non-structural proteins including Papain-like protease (nsp3) formed by the cleavage of polyprotein along with other components. In **Figure 2B**, the 3D structure of PLpro with Famotidine (red color) in the binding site can be seen.

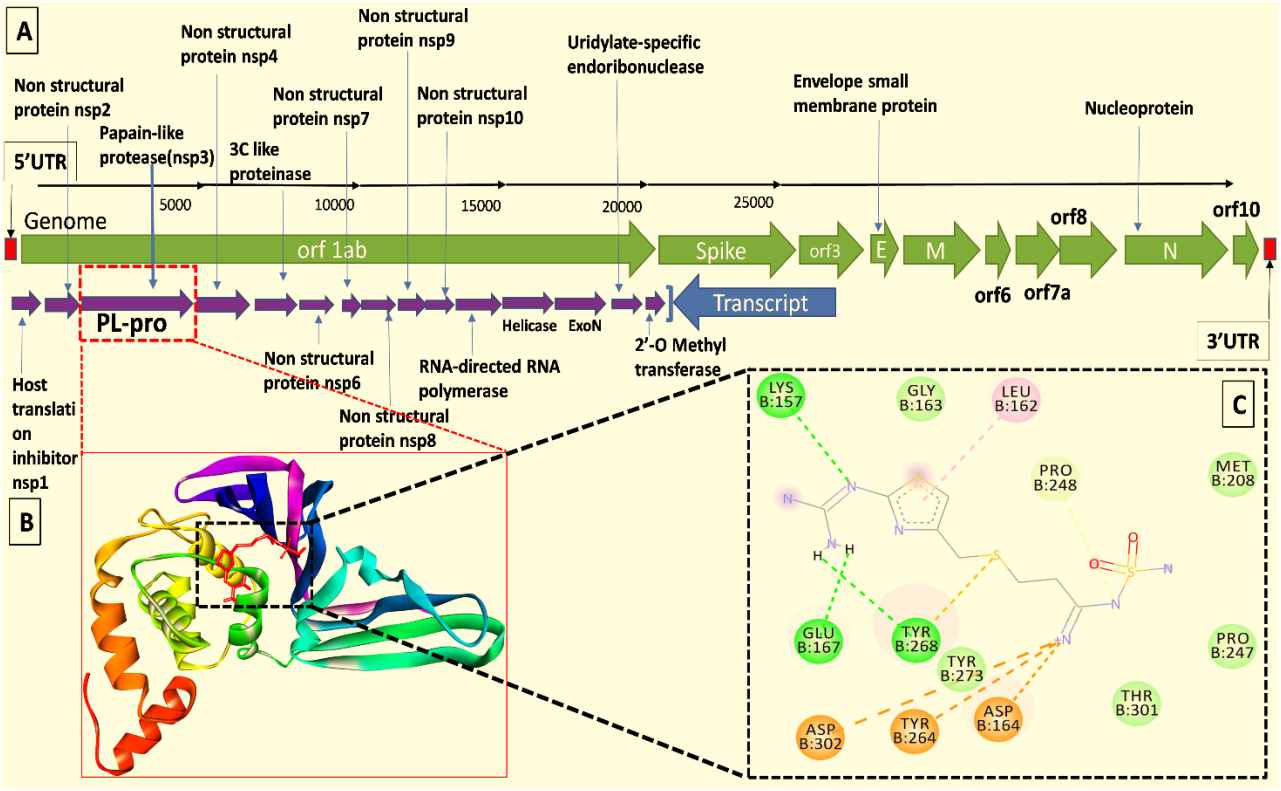

Figure 2: (A) The single-stranded RNA genome of SARS-CoV-2, (B) the 3D structure of the PLpro-Famotidine complex, and (C) the 2D plot of the amino acid residues of PLpro interacting with the Famotidine drug.

Hydrogen bonding, van der Waals, and Π interactions (Π-Cation, Π-Sulfur, Π-Alkyl) are the major contributors towards the stability and binding energy of the PLpro-Famotidine complex (**Figure 2C**). Amino acid residues LYS157, GLU167, and TYR268 are involved in the formation of three hydrogen bonds. Residues GLY163, MET208, PRO247, TYR273, and THR301 are

involved in the van der Waals interaction. Residue LEU162 forms Π-alkyl and TYR268 which was involved in hydrogen bonding also forms Π-Sulfur bond. Π-Cation bond is formed by ASP164, TYR264, and ASP302 residues. There are thirteen amino acid residues involved in the interaction with Famotidine in which TYR268 seems to be the most crucial one for the stability as it is associated with both hydrogen bond as well as Π-Sulfur bond formation. Earlier, it was also noticed that the conserved amino acid residue TYR268 had a critical role in the inhibitory action of GRL–0617 to PLpro of SARS-CoV-2 (Shin et al., 2020) which corroborates with our result.

3.2 MD trajectory analysis

MD simulations have great significance to scrutinize the internal motions, conformational changes, stability, etc. of protein-ligand complexes and are shown to be effective in inhibitor designing and mutational analysis (Sen Gupta et al., 2020; Singh et al., 2020). Using the generated MD trajectories, the root-mean-square deviation (RMSD), root-mean-square fluctuation (RMSF), radius of gyration (Rg), hydrogen bonding (HB), and principal component analysis (PCA) were computed and the results are discussed below.

RMSD is an essential structural and dynamical parameter to investigate the conformational stability despite allowing to assess the quality, equilibration, and convergence of an MD run (Sen Gupta et al., 2020). A larger RMSD value is indicative of the lower stability of a protein complex and vice-versa. In this study, the RMSD of the PLpro-Famotidine complex and PLpro without ligand with respect to the Cα atom was calculated against the MD simulation time which is shown in the **Figure 3A**. In the case of the PLpro without ligand, the average RMSD is around 0.3 nm, with fluctuations at around 5 ns and 40 ns (Figure 3A). Whereas, in the case of the PLpro-Famotidine complex, the average RMSD is around 2.9 nm and slight fluctuation has been seen at 44 ns and remains stable during the rest of the simulation period. The lower average value and lesser fluctuation of the RMSD of PLpro in complex similar to the unbound PLpro suggest stability of the target-drug complex and hence a strong bonding between the two.

Similarly, **RMSF** is a useful parameter that estimates residue flexibility during dynamics with respect to the backbone atoms of each amino acid residue of PLpro in the complex and unbound state presented in **Figure 3B**. In the case of PLpro without ligand, the average RMSF is around 2.7 nm, and apart from the starting and terminal residues, higher spikes could be seen at the

residues 105, 155, 190, 199, 226, and 262 as shown in the plot of **Figure 3B**. Likewise, in the case of the PLpro-Famotidine complex, with the average RMSF of 2.6 nm, often spikes appear in the RMSF plot at the same locations as before (**Figure 3B**), which is consistent with the RMSD analysis for inferring the stability of the bound state.

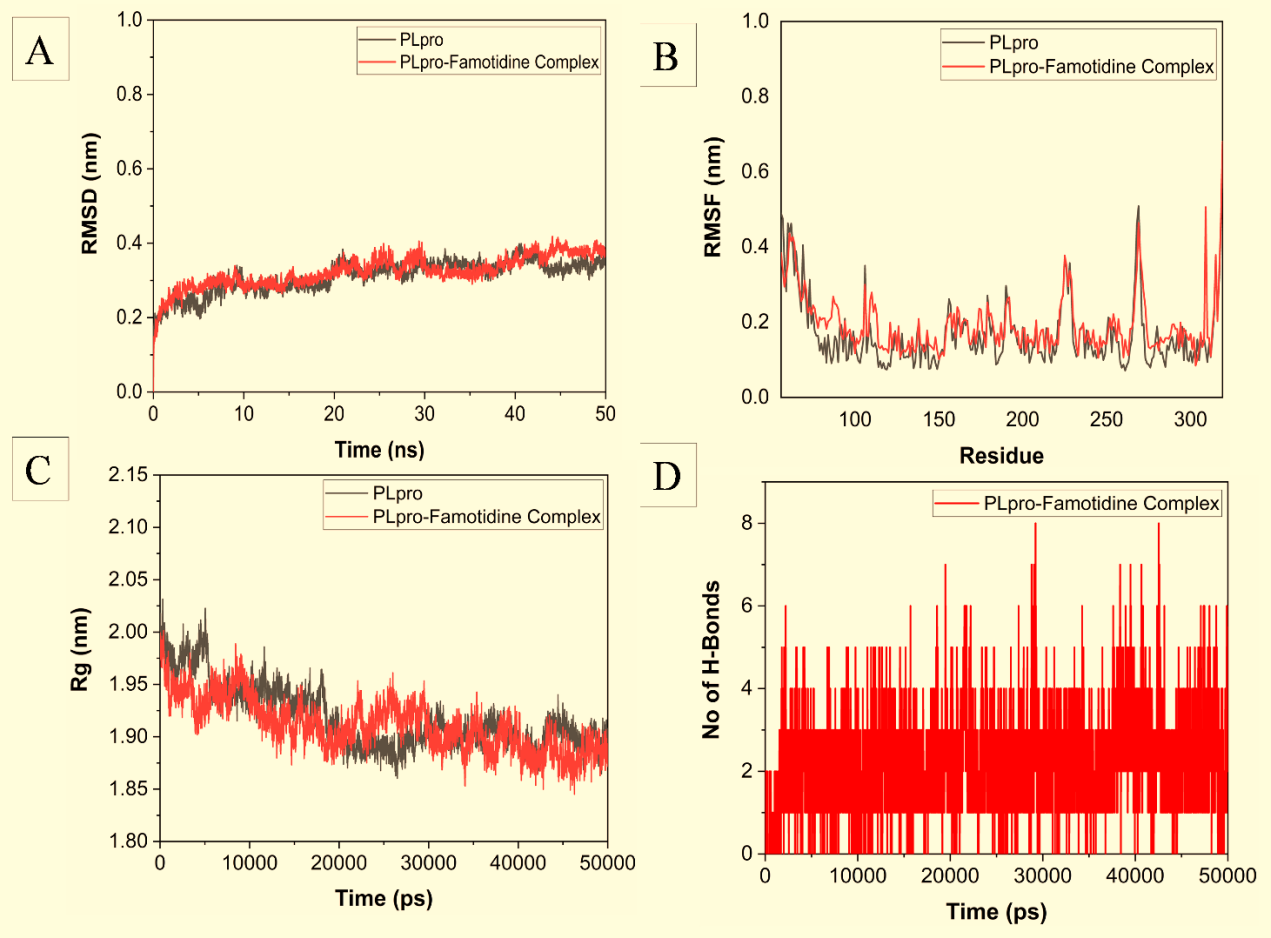

Figure 3: Plots of (A) RMSD as a function of simulation time, (B) RMSF as a function of amino acid residues, (C) R_g as a function of simulation time, and (D) the average number of hydrogen bonds as a function of simulation time for PLpro without ligand (Black color) and in the PLpro-Famotidine complex (Red color)

The **radius of gyration** (R_g) describes the level of compaction of protein. It is defined as the mass-weighted root-mean-square distance for a collection of atoms from their common center of mass. Hence, the trajectory analysis for the radius of gyration depicts the evolution of the overall dimension of protein during dynamics. In the case of PLpro without ligand, the average

value of R_g is 1.94 nm and there is a large fall at around 25 ns (**Figure 3C**). On the other hand, in the case of the PLpro-Famotidine complex, the average value of R_g is around 1.93 nm and there occurs similar decay in the R_g plot as shown in **Figure 3C**. During most of the time span of MD, PLpro without ligand and in the complex is observed to be stable as no large fluctuations observed; the protein is stable in the complex as well as it is evident.

The existence of **Hydrogen bond** interaction is important for the stability of a protein complex. A greater number of intermolecular hydrogen bonds can endow larger stability to a protein complex. As observed during the MD simulation (see **Figure 3D**), the average number of hydrogen bonds of the PLpro-Famotidine complex is three which interestingly corroborates with the result of molecular docking (hydrogen bond formed by three residues: LYS157, GLU167, and TYR268) (**Figure 2C**).

Compared to the unbound state, PLpro in the complex rather exhibit a lower average value or fluctuation in all of the above cases. Altogether, the analysis of the RMSD, RMSF, Rg, and the number of hydrogen bonds indicates the stability of the PLpro-Famotidine complex validating the preliminary docking result as there is no appreciable difference between the bound and unbound states.

3.3 Principal component analysis (PCA)

The molecular dynamics trajectories were used for PCA to identify the conformational motions relevant to protein functions. Eigenvalues were used to calculate the conformational changes due to the movement of atoms (Khan et al., 2016). The eigenvalues were generated by diagonalizing the covariance matrix of the Cα atomic fluctuations against the equivalent Eigenvectors' (EV) indices. The first 10 modes were taken into consideration in the analysis of the essential subspace as they cover >95% variance of the protein where an exponentially decaying curve of eigenvalues is obtained against the EVs (**Figure 4A**). In this study, PC1 and PC2 that dominate the protein conformational fluctuations were also used for the analysis of PLpro without ligand and in the famotidine complex.

Taken the first two PCs into consideration, simulation results revealed the subspace dimension for PLpro in the unbound state and in the complex is comparable, with no noticeable large

difference in the dimension(**Figure 4B**). This is also reflected in their 2D projection plots of trajectories, with similar trace values of the covariance matrix for both.

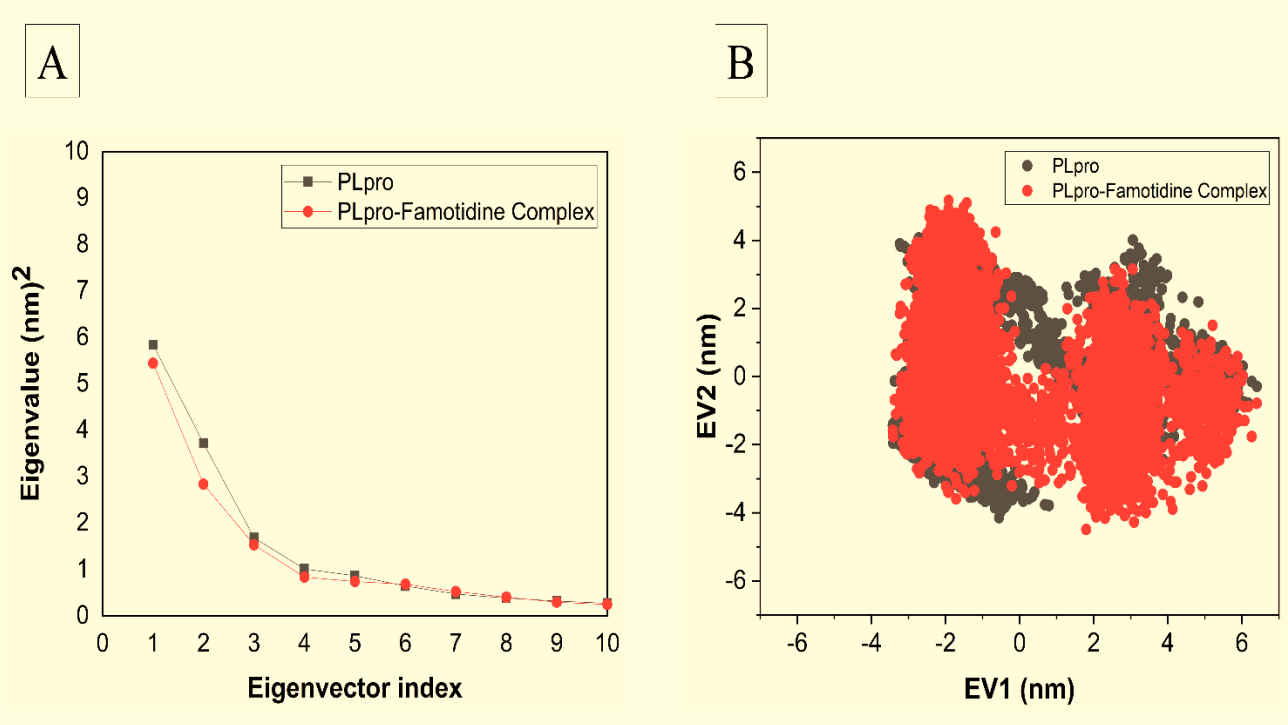

Figure 4: Principal component analysis (PCA) of PLpro in the unbound state (Black color) and in the PLpro-Famotidine complex (Red color): (A) the plot of eigen values versus the corresponding eigen vector indices coming from the C_α covariance matrix during MD simulations and (B) the 2D projection plot of the first two principal eigenvectors.

The overall analysis manifests again that the PLpro-Famotidine complex has retained its stability as reflected from its least conformational changes due to decreasing collective motions from the unbound state of PLpro.

4. Conclusion

Famotidine is an FDA-approved drug and reported to have improved clinical outcomes and the reduced risk of intubation or death when used in the 1,620 hospitalized patients of COVID-19. In this study, the analysis of molecular docking study revealed that out of twelve targets, PLpro has the highest binding affinity with clinically effective drug Famotidine. Further, the results of the root-mean-square deviation after MD simulations of the complex and PLpro suggest the stability of the PLpro-Famotidine complex. Similarly, the root-mean-square deviation, radius of

gyration, and PCA also corroborate with the result. Overall, the present computational study identifies the Papain-like protease (PLpro) as the most probable target for the FDA approved drug Famotidine providing necessary information for further experimental exploration, which can proliferate the design of more potential therapeutics against the identified SARS-CoV-2 target.

Acknowledgements

The authors acknowledge IISER Berhampur for computational support. P.S.S.G also sincerely acknowledges IISER Berhampur for providing him the Institute Postdoc Fellowship to carry out this work.

Conflict of interest

The authors report no conflicts of interest.

References

Bourinbaiar AS, Fruhstorfer EC**.** The effect of histamine type 2 receptor antagonists on human immunodeficiency virus (HIV) replication: identification of a new class of antiviral agents. Life Sci. 1996;59(23):PL 365-70. doi: 10.1016/s0024-3205(96)00553-x

Cao YC, Deng QX, Dai SX. Remdesivir for severe acute respiratory syndrome coronavirus 2 causing COVID-19: An evaluation of the evidence. Travel Medicine and Infectious Disease. 2020 Apr 2:101647. doi: 10.1016/j.tmaid.2020.101647

Chang, C., Sue, S.-C., Yu, T., Hsieh, C.-M., Tsai, C.-K., Chiang, Y.-C., Lee, S., Hsiao, H., Wu, W.-J., Chang, W.-L., Lin, C.-H., & Huang, T. (2006). Modular organization of SARS coronavirus nucleocapsid protein. *Journal of Biomedical Science*, *13*(1), 59–72. https://doi.org/10.1007/s11373-005-9035-9

Cucinotta D, Vanelli M. WHO declares COVID-19 a pandemic. Acta bio-medica: Atenei Parmensis. 2020 Mar 19;91(1):157-60. doi: 10.23750/abm.v91i1.9397

Essmann, L. Perera, M. L. Berkowitz, T. Darden, H. Lee, L. G. Pedersen, 1995. A smooth particle mesh Ewald method. *The Journal of Chemical Physics*, 103, 8577-8593. 10.1063/1.470117

Freedberg, Daniel E., et al. "Famotidine Use is Associated with Improved Clinical Outcomes in Hospitalized COVID-19 Patients: A Retrospective Cohort Study." *medRxiv* (2020). doi: https://doi.org/10.1101/2020.05.01.20086694

Gupta MK, Vemula S, Donde R, Gouda G, Behera L, Vadde R. In-silico approaches to detect inhibitors of the human severe acute respiratory syndrome coronavirus envelope protein ion channel. Journal of Biomolecular Structure and Dynamics. 2020 Apr 2(just-accepted):1-7. https://doi.org/10.1080/07391102.2020.1751300

Hess U, Blairy S, Kleck RE. The intensity of emotional facial expressions and decoding accuracy. Journal of Nonverbal Behavior. 1997 Dec 1;21(4):241-57. DOI:10.1023/A:1024952730333

Khan, M. Garg, Q. Gui, M. Schadt, A. Gaikwad, D. Han,A. C. Arias, 2016. Flexible Hybrid Electronics: Direct Interfacing of Soft and Hard Electronics for Wearable Health Monitoring. *Advanced Functional Materials*, 26, 8764-8775. https://doi.org/10.1002/adfm.201603763

Kong R, Yang G B, Xue R, Liu M, Wang F, Hu J P, Guo X Q, Chang S. COVID-19 Docking Server: An interactive server for docking small molecules, peptides and antibodies against potential targets of COVID-19. 2020. arXiv:2003.00163v1 [q-bio.BM].

Kiemer, Lars, et al. "Coronavirus 3CL pro proteinase cleavage sites: Possible relevance to SARS virus pathology." *BMC bioinformatics* 5.1 (2004): 72. doi: 10.1186/1471-2105-5-72

Li, Guangdi, and Erik De Clercq. "Therapeutic options for the 2019 novel coronavirus (2019-nCoV)." (2020): 149-150. DOI: 10.1038/d41573-020-00016-0

Muralidharan N, Sakthivel R, Velmurugan D, Gromiha MM. Computational studies of drug repurposing and synergism of lopinavir, oseltamivir and ritonavir binding with SARS-CoV-2 Protease against COVID-19. Journal of Biomolecular Structure and Dynamics. 2020 Apr 4(just-accepted):1-7. https://doi.org/10.1080/07391102.2020.1752802

Oostenbrink, A. Villa, A. E. Mark, W. F. Van Gunsteren, 2004. A biomolecular force field based on the free enthalpy of hydration and solvation: The GROMOS force-field parameter sets 53A5 and 53A6. *Journal of Computational Chemistry*, 25, 1656-1676. DOI: 10.1002/jcc.20090

Petropoulos F, Makridakis S. Forecasting the novel coronavirus COVID-19. PloS one. 2020 Mar 31;15(3):e0231236. https://doi.org/10.1371/journal.pone.0231236

Prajapat, M., Sarma, P., Shekhar, N., Avti, P., Sinha, S., Kaur, H., Kumar, S., Bhattacharyya, A., Kumar, H., Bansal, S., & Medhi, B. (2020). Drug targets for corona virus: A systematic review. *Indian Journal of Pharmacology*, *52*(1), 56. https://doi.org/10.4103/ijp.IJP_115_20

Pronk, S. Páll, R. Schulz, P. Larsson, P. Bjelkmar, R. Apostolov, E. Lindahl, 2013. GROMACS 4.5: a high-throughput and highly parallel open source molecular simulation toolkit. *Bioinformatics*, 29, 845-854. doi: 10.1093/bioinformatics/btt055

Ratia, Kiira, et al. "Severe acute respiratory syndrome coronavirus papain-like protease: structure of a viral deubiquitinating enzyme." *Proceedings of the National Academy of Sciences* 103.15 (2006): 5717-5722. doi: 10.1073/pnas.0510851103

Sarma P, Sekhar N, Prajapat M, Avti P, Kaur H, Kumar S, Singh S, Kumar H, Prakash A, Dhibar DP, Medhi B. In-silico homology assisted identification of inhibitor of RNA binding against

2019-nCoV N-protein (N terminal domain). Journal of Biomolecular Structure and Dynamics. 2020 Apr 7(just-accepted):1-1. https://doi.org/10.1080/07391102.2020.1753580

Schenone, Monica et al. “Target identification and mechanism of action in chemical biology and drug discovery.” *Nature chemical biology* vol. 9,4 (2013): 232-40. doi:10.1038/nchembio.1199

Sekiguchi T, Nishioka T, Kogure M et al. Once-daily administration of famotidine for reflux esophagitis. *Scand J Gastroenterol*. 1987; 22(Suppl 134):51-4.

Sen Gupta PS, Islam RN, Banerjee S, Nayek A, Rana MK, Bandyopadhyay AK. Screening and molecular characterization of lethal mutations of human homogentisate 1, 2 dioxigenase. Journal of Biomolecular Structure and Dynamics. 2020 Mar 14:1-1. doi: 10.1080/07391102.2020.1736158

Shaffer, L. "15 drugs being tested to treat COVID-19 and how they would work." *Nature medicine* (2020).

Shin D, Mukherjee R, Grewe D, Bojkova D, Baek K, Bhattacharya A, Schulz L, Widera M, Mehdipour AR, Tascher G, Geurink PP. Inhibition of papain-like protease PLpro blocks SARS-CoV-2 spread and promotes anti-viral immunity. DOI: 10.21203/rs.3.rs-27134/v1

Singh VK, Srivastava R, Sen Gupta PS, Naaz F, Chaurasia H, Mishra R, Rana MK, Singh RK. Anti-HIV potential of diarylpyrimidine derivatives as non-nucleoside reverse transcriptase inhibitors: Design, synthesis, docking, TOPKAT analysis and molecular dynamics simulations. Journal of Biomolecular Structure and Dynamics. 2020 Mar 27(just-accepted):1-8. doi: 10.1080/07391102.2020.1748111

Trott O, Olson AJ. AutoDock Vina: improving the speed and accuracy of docking with a new scoring function, efficient optimization, and multithreading. Journal of computational chemistry. 2010 Jan 30;31(2):455-61. doi: 10.1002/jcc.21334

Wishart,D.S., Feunang,Y.D., Guo,A.C., Lo,E.J., Marcu,A., Grant,J.R., & Assempour,N.(2018).DrugBank5.0:a major update to the Drug Bank database for 2018. Nucleic acids research, 46(D1), D1074-D1082.doi:10.1093/nar/gkx1037

Wu C, Liu Y, Yang Y, Zhang P, Zhong W, Wang Y, Wang Q, Xu Y, Li M, Li X, Zheng M. Analysis of therapeutic targets for SARS-CoV-2 and discovery of potential drugs by computational methods. Acta Pharmaceutica Sinica B. 2020 Feb 27. https://doi.org/10.1016/j.apsb.2020.02.008

Zhu, N., Zhang, D., Wang, W., Li, X., Yang, B., Song, J., Zhao, X., Huang, B., Shi, W., Lu, R., Niu, P., Zhan, F., Ma, X., Wang, D., Xu, W., Wu, G., Gao, G. F., & Tan, W. (2020). A Novel Coronavirus from Patients with Pneumonia in China, 2019. *New England Journal of Medicine*. https://doi.org/10.1056/NEJMoa2001017